International Journal of
Mathematical Modelling & Computations
Vol. 14, No. 03, Summer 2024, 187- 199
DOI:10.71932/ijm.2024.1195092

Collocation Method for Solving Systems of Fractional Differential Equations, A Case Study of HIV Infection by Using Müntz Wavelets Basis

Maryam Bahmanpour[a,*]

[a] *Department of Mathematics, Isfahan(Khorasgan) Branch, Islamic Azad University, Isfahan, Iran*

Abstract. The primary objective of this study is to solve a system of fractional differential equations using Müntz wavelets. In this approach, the Müntz wavelets are appropriately modified through the incorporation of polynomials. The error associated with the proposed method is thoroughly analyzed and evaluated. This methodology is specifically applied to the fractional form of the HIV infection model. The numerical results obtained further substantiate the efficacy and accuracy of the proposed method.

Received: 04 May 2024, Revised: 20 July 2024, Accepted: 24 July 2024.

Keywords: Müntz wavelels; Fractional differential equations systems;Collocation method; Jacobi polynomials; HIV infection.

AMS Subject Classification:

Index to information contained in this paper

1. Introduction

Wavelets are powerful and practical tools that have been extensively used for solving both integral and differential equations across various domains. Numerous types of wavelets have been introduced for this purpose, including Haar wavelets [2], Legendre wavelets [18], and Chebyshev wavelets of the first, second, third, and fourth kinds [3, 4, 9], among others. In essence, wavelets serve as orthogonal bases that

*Corresponding author. Email: mbahmanpour@yahoo.com

are widely applied not only to solve integral and differential equations but also to address a variety of problems in mathematics, engineering, and medicine. While Haar wavelets are computationally simple due to their relatively low number of operations, they are often less accurate when applied to complex problems. On the other hand, Legendre wavelets, with the weight function $w(x) = 1$, are recognized for their simplicity and low computational cost, offering relatively good accuracy in a broad range of problems. Chebyshev wavelets, which are characterized by their weight functions, generally involve more computational operations. However, in the context of integral equations where the kernel is inversely proportional to the weight function, Chebyshev wavelets exhibit remarkable accuracy. This article intends to introduce the Müntz wavelet and examine its application. An important difference of Müntz wavelet and above-mentioned ones is the degree of the extended sentences. For more explanation, all the former wavelets are in the form of

$$\Sigma_{i=1}^{\infty} c_i x^i,$$

while the form of the Müntz wavelet is as follows:

$$\Sigma_{i=1}^{\infty} c_i x^{\lambda_i},$$

in which λ_i is a complex number. So it can be argued that, Müntz wavelet not only gives a good approximation for fractional power and complex functions, but also covers a wide range of functions. Fractional calculus first emerged as a pure mathematical theory in the mid-nineteenth century. [22].One hundred years later, engineers and physicists faced practical problems with fractional arithmetic [13**?**]. A good way to describe the memory and hereditary properties of different materials and processes is to use fractional derivatives. [25]. In some cases, fractional order models of real systems perform better than correct order ones. To illustrate, researchers have used fractional derivatives in many fields related to science and engineering, including fluid flow, rheology, diffusion-like diffusion, electrical networks, electromagnetic theory, and probability. [14, 17, 21**?**]. Most of these equations do not have exact analytical answers.This forces us to use approximate and numerical techniques. So far, several analytical and numerical methods for solving fractional differential equations have been proposed. As the main examples one can mention to domain decomposition method [8], Linear B-spline method [16], Product integration method [12], multistep method [11], Predictor Corrector method [**?**], Extrapolation method [7]. In this paper, we present an approximate solution for a system of differential equations in $t \in [0, T]$. The general form of this type of equation is as follows:

$$\begin{cases} D_*^{\omega_1} y_1(t) = g_1(t, y_1(t), y_2(t), \ldots, y_n(t)) \\ D_*^{\omega_2} y_2(t) = g_2(t, y_1(t), y_2(t), \ldots, y_n(t)) \\ \vdots \\ D_*^{\omega_n} y_n(t) = g_n(t, y_1(t), y_2(t), \ldots, y_n(t)) \\ y_i(0) = \mu_i \end{cases} \quad 0 < \omega_i < 1, i = 1, 2, \ldots, n. \tag{1}$$

Where $D_*^{\omega_i} y_i(t)$ and g_i are respectively the fractional derivative of order ω_i and function by t and $y_i(t)$ and μ_i are known constant number. The aim of solving this equation is the calculation of $y_i(t)$.

In the present study, the first stage involves the introduction of Müntz wavelets. These wavelets are demonstrated to be faster and more accurate than Müntz Legendre polynomials. In the second stage, Müntz Legendre polynomials are introduced within the interval $[0,1]$. Following these stages, the definitions and properties of wavelets are thoroughly discussed. The presentation then extends to Müntz wavelets within the range $[0,T]$. Utilizing Jacobi polynomials, a more stable formulation for Müntz wavelets is subsequently developed. Finally, fractional differential equations are solved, accompanied by an error analysis review. To assess the accuracy of the proposed method, both mathematical and practical examples are provided.

2. Müntz Legendre polynomials

Assume that the set $\Lambda_n = \{\lambda_1, \lambda_2, ..., \lambda_n\}$ is a sequence of complex numbers, provided that $Re(\lambda_k > -1/2)$. So one can define Müntz Legendre polynomials in the interval $[0,1]$ as follows [24]:

$$L_n(x) = L_n(x, \Lambda_n) = \Sigma_{k=0}^{n} c_{n,k} x^{\lambda_k}, \tag{2}$$

$$c_{n,k} = \frac{\prod_{v=0}^{n-1} \lambda_k + \overline{\lambda}_v + 1}{\prod_{v=0, v\neq k}^{n-1} \lambda_k - \lambda_v}. \tag{3}$$

These polynomials are orthogonal with respect to the weight function $w(x) = 1$. As a result, one can say that:

$$(L_n(x), L_m(x)) = \int_0^T L_n(x) L_m(x) dx = \frac{\delta_{m,n}}{\lambda_n + \overline{\lambda}_{n+1}}. \tag{4}$$

Where $(.,.)$ represents the inner product and $\delta_{m,n}$ is Kronecker delta function. In this work, it assumes that $\lambda_k = \gamma k$, then

$$L_n(x) = L_n(x, \gamma) = \Sigma_{k=1}^{n} c_{n,k} x^{\gamma_k}, \tag{5}$$

$$c_{n,k} = \frac{(-1)^{n-k}}{\gamma^n k!(n-k)!} \prod_{v=0}^{n-1} ((k+v)\gamma + 1). \tag{6}$$

3. Wavelets

Wavelet families are generated through the scaling and translation of a fundamental function known as the mother wavelet. By continuously varying the scaling and translation parameters, different continuous wavelet families emerge [10]:

$$\psi_{a,b}(t) = |a|^{-1/2} \psi(\frac{t-b}{a}), a, b \in R, a \neq 0.$$

Where a and b are expansion and transfer parameters, respectively.
If the parameters a and b are bound to discrete values, i.e. $b_0 > 0, a_0 > 1, a = a_0^{-k}, b = n b_0 a_0^{-k}$ and if n is a positive integer number:

$$\psi_{a,b}(t) = |a_0|^{k/2} \psi(a_0^k t - n b_0).$$

Thus the following discrete wavelet family is formed:

$$\psi_{k,n}(t) = |a_0|^{k/2}\psi(a_0^k t - nb_0). \tag{7}$$

Where $\psi_{k,n}(t)$is a basic wavelet for $L^2(R)$.
In general, if one assumes that $a_0 = 2$ and $b_0 = 1$, then $\psi_{k,n}(t)$ produces an orthonormal basis.

3.1 *Müntz wavelets*

Consider Müntz Legendre's polynomial of degree m is denoted by $L_m(x,\gamma)$.These polynomials are orthogonal to their weight function $w(t) = 1$. Müntz wavelets have four arguments $\psi_{n,m}(t) = \psi(k,n,m,t)$ in which $m = 0,1,...,M-1$, $n = 1,2,...,2^{k-1}$ and $k = 2,3,\ldots$ (M is a positive integer number).
Eq. (8) shows a definition of the Müntz wavelets on $[0,T]$:

$$\psi_{n,m}(t) = \begin{cases} \sqrt{2^{k-1}(1+2m\gamma)}L_m[2^{k-1}t - T(n-1),\gamma], & \frac{(n-1)T}{2^{k-1}} \leqslant t < \frac{nT}{2^{k-1}} \\ 0, \quad otherwise. \end{cases} \tag{8}$$

In Eq. (8), increasing M value causes the coefficients increase and become very large. However, the sum of the coefficients is always equal to $\sqrt{2^{k-1}(1+2m\gamma)}$.
In the next section it is shown that Müntz wavelets can be obtained using Jacobi polynomials in such a way that the wavelet coefficients to be stabilized.

3.2 *Jacobi polynomials*

Jacobi polynomials with the weight function $w(x) = (1-x)^\alpha(1+x)^\beta$ and $\alpha,\beta > -1$ are orthogonal. They are defined as follows [5, 24]:

$$J_k^{\alpha,\beta}(x) = \sum_{m=0}^{k} \frac{(-1)^{k-m}(1+\beta)^k(1+\alpha+\beta)^{k+m}}{m!(k-m)!(1+\beta)^m(1+\alpha+\beta)^k}(\frac{1+x}{2})^m, x \in [-1,1]. \tag{9}$$

Also, one can say that:

$$\begin{cases} J_0^{\alpha,\beta}(x) = 1 \\ J_1^{\alpha,\beta}(x) = \frac{1}{2}((\alpha-\beta)+(\alpha+\beta+2)x) \\ J_{k+1}^{\alpha,\beta}(x) = \frac{b_k^{\alpha,\beta}(x)}{a_k^{\alpha,\beta}}J_k^{\alpha,\beta}(x) - c_k^{\alpha,\beta}J_{k-1}^{\alpha,\beta}(x). \end{cases} \tag{10}$$

Where

$$\begin{cases} a_k^{\alpha,\beta} = 2(k+1)(k+\alpha+\beta+1)(2k+\alpha+\beta) \\ b_k^{\alpha,\beta}(x) = (2k+\alpha+\beta+1)((2k+\alpha+\beta)(2k+\alpha+\beta+2)x+\alpha^2-\beta^2) \\ c_k^{\alpha,\beta} = 2(k+\alpha)(k+\beta)(2k+\alpha+\beta+2). \end{cases} \tag{11}$$

Then, using Jacobi polynomials, we introduce the modified Müntz wavelets.

3.3 *Modified Müntz wavelets*

Theorem 3.1 Assuming that $J_m^{\alpha,\beta}(x)$ is a Jacobi polynomial of degree m, with $\alpha > 0$ being a real number and $t \in [0, T]$, we can then rewrite Eq. (8) as follows:

$$\psi_{n,m}(t) = \begin{cases} \sqrt{2^{k-1}(1+2m\gamma)} J_m^{(0,\frac{1}{\gamma}-1)}\left(2\left(\frac{(2^{k-1}t - T(n-1))}{T}\right)^{\gamma} - 1\right), \frac{(n-1)T}{2^{k-1}} \leqslant t < \frac{nT}{2^{k-1}} \\ 0, \quad otherwise. \end{cases} \tag{12}$$

Proof. According to the Eq. (8) and Eq. (12), it suffices to show that:

$$L_m[2^{k-1}t - T(n-1), \gamma] = J_m^{(0,\frac{1}{\gamma}-1)}\left(2\left(\frac{(2^{k-1}t - T(n-1))}{T}\right)^{\gamma} - 1\right),$$
$$\frac{(n-1)T}{2^{k-1}} \leqslant t < \frac{nT}{2^{k-1}}.$$

With the change of variables $x = 2^{k-1}t - T(n-1)$ we have:

$$L_m[x, \gamma] = J_m^{(0,\frac{1}{\gamma}-1)}\left(2(\frac{x}{T})^{\gamma} - 1\right), \quad 0 \leqslant t < 1.$$

Putting $y = 2(\frac{x}{T})^{\gamma} - 1$ in Eq. (9):

$$J_m^{(0,\frac{1}{\gamma}-1)}\left(2(\frac{x}{T})^{\gamma} - 1\right) = \sum_{k=0}^{m} \frac{(-1)^{m-k}(\frac{1}{\gamma})^m(\frac{1}{\gamma})^{m+k}}{k!(m-k)!(\frac{1}{\gamma})^m(\frac{1}{\gamma})^k}(\frac{x}{T})^{k\gamma}$$
$$= \sum_{k=0}^{m} c_{m,k}(\frac{x}{T})^{k\gamma} = L_m(x, \gamma). \blacksquare$$

Now, with respect to Theorem 1 and Eq. (10) and Eq. (11), the modified wavelet Müntz will be as follows:

$$\psi_{n,m}(t) = \begin{cases} \sqrt{\frac{2^{k-1}(1+2m\gamma)}{T}} \widetilde{L}_m[2^{k-1}t - T(n-1)), \gamma], \quad \frac{(n-1)T}{2^{k-1}} \leqslant t < \frac{nT}{2^{k-1}} \\ 0, \quad otherwise. \end{cases} \tag{13}$$

Where $\widetilde{L}_m$ is the Müntz modified formula:

$$\begin{cases} \widetilde{L}_0(x, \gamma) = 1 \\ \widetilde{L}_1(x, \gamma) = (\frac{1}{\gamma} + 1)(\frac{x}{T})^{\gamma} - \frac{1}{\gamma} \\ \widetilde{L}_{m+1}(x, \gamma) = \frac{1}{a_m}\left(b_m(x)\widetilde{L}_m(x, \gamma) - c_m \widetilde{L}_{m-1}(x, \gamma)\right), \end{cases} \tag{14}$$

in which

$$\begin{cases} a_m = a_m^{(0,\frac{1}{\gamma}-1)} \\ b_m(x) = b_m^{(0,\frac{1}{\gamma}-1)}\left(2\left(\frac{x}{T}\right)^{\gamma} - 1\right) \\ c_m = c_m^{(0,\frac{1}{\gamma}-1)}. \end{cases} \tag{15}$$

As previously mentioned, the coefficients in Eq. (8) grow significantly as m increases. However, the sum of these coefficients is consistently equal to

$\sqrt{2^{k-1}(1+2m\gamma)}$. In fact, by applying Eq. (5) and calculating $L_m(1) = L_m(1,\gamma) = \sum_{k=1}^{m} c_{m,k}$, we can confirm that the sum of the coefficients in $\psi_{n,m}(t)$ remains constant and equals $\sqrt{2^{k-1}(1+2m\gamma)}$. For instance, for $k = 1$, $m = 5$ and $\gamma = 0.5$, using Eq. (8) gives:

$$\psi_{1,5}(t) = \sqrt{6}\left(-6 + 105t^{1/2} - 560t + 1260t^{3/2} - 1260t^2 + 462t^{5/2}\right), \quad 0 \leqslant t < 1.$$

On the other hand, using (13), we can write $\psi_{1,5}(t)$ differently,

$$\begin{aligned}\psi_{1,5}(t) = {} & \frac{1}{90\sqrt{6}}(\frac{1}{28}(\frac{1}{15}(-1+63(-1+2\sqrt{t})(\frac{1}{6}(-1+35(-1+2\sqrt{t}))(-20+4(-1\\ & +15(-1+2\sqrt{t}))(-2+3\sqrt{t})) - 84(-2+3\sqrt{t})) - 6(-20+4(-1\\ & +15(-1+2\sqrt{t}))(-2+3\sqrt{t})))(-1+99(-1+2\sqrt{t})) - \frac{11}{3}(\frac{1}{6}(-1\\ & +35(-1+2\sqrt{t}))(-20+4(-1+15(-1+2\sqrt{t}))(-2+3\sqrt{t}))\\ & -84(-2+3\sqrt{t}))), \qquad\qquad 0 \leqslant t < 1.\end{aligned}$$

It has been observed that in the modified formula (13), large coefficients do not appear. To highlight the difference between (8) and (13) in the numerical evaluation of Müntz wavelets, the values of $\psi_{1,m}(t)$ for selected values of t, with $\gamma = 1/2$, $k = 2$ and $m = 20, 40, 50$, are provided in Table 1.As shown in the table, the values calculated using (8) for $m = 40$ and 50 exhibit a significant error rate, except when t is very close to zero. Furthermore, the sum of the coefficients is given by $\psi_{n,m}(\frac{n}{2^{k-1}}) = \sqrt{2^{k-1}(1+2m\gamma)}$, which ensures that at the endpoint of each section, specifically at $t = \frac{n}{2^{k-1}}$, the exact values of $\psi_{n,m}(t)$ are known. Figure 1 illustrates the absolute errors of $\psi_{1,m}(0.5)$ for $\gamma = 1/2$, $k = 2$, and various values of m, using the formulas (8) and (13).

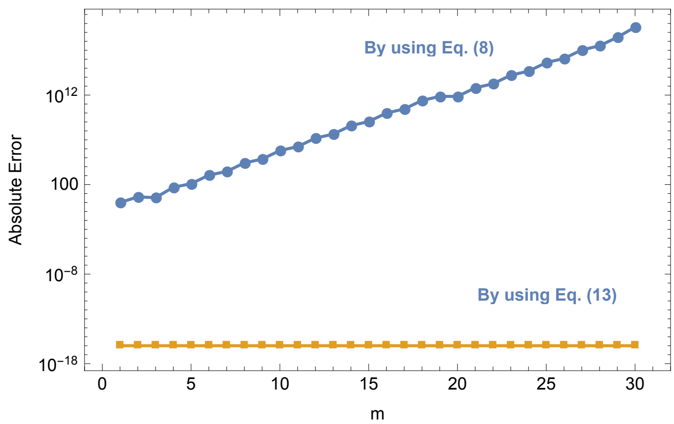

Figure 1. Absolute errors in the values $\psi_{1,m}(1/2)$ for $\gamma = 1/2$, $k = 2$ and various values of m.

Table 1. Calculated values of $\psi_{1,m}(t)$ for $\gamma = 1/2$, $k = 2$ and $m = 20, 40, 50$.

	$m = 20$		$m = 40$		$m = 50$	
t	Eq. (8)	Eq. (13)	Eq. (8)	Eq. (13)	Eq. (8)	Eq. (13)
0.0005	5.061460	5.061460	10.4346	10.4346	-10.5350	-10.5350
0.005	0.868465	0.868465	2.12626	2.12626	2.70601	2.70945
0.05	-1.521720	-1.521720	-144.886	-1.82540	-2.11802×10^7	-0.89844
0.25	-0.470313	-0.468590	-2.67387×10^{10}	-0.73353	-1.33610×10^{17}	0.77026
0.45	-1.499940	-1.411100	6.96955×10^{13}	1.07803	9.48981×10^{20}	-1.50813
0.49	-2.506220	-2.445380	-5.97390×10^{13}	1.03524	-5.23977×10^{21}	-2.53715

4. Error assessment:

To check syntactic error analysis, let $y_L(t)$ is the approximate solution obtained from Eq. (2).

$$y_L(t) = (\widetilde{y}_1(t), \widetilde{y}_2(t), \ldots, \widetilde{y}_N(t)) = (\sum_{j=0}^{L} a^1_{n,j}\psi_{n,j}(t), \sum_{j=0}^{L} a^2_{n,j}\psi_{n,j}(t), \ldots, \sum_{j=0}^{L} a^N_{n,j}\psi_{n,j}(t)),$$

and $y(t)$ is the exact solution:

$$y(t) = (y_1(t), y_2(t), \ldots, y_N(t)) = (\sum_{j=0}^{\infty} a^1_{n,j}\psi_{n,j}(t), \sum_{j=0}^{\infty} a^2_{n,j}\psi_{n,j}(t), \ldots, \sum_{j=0}^{\infty} a^N_{n,j}\psi_{n,j}(t)),$$

then we have:

$$\begin{cases} D^{\omega}_{*}\widetilde{y}_1(t) = g_1(t, \widetilde{y}_1(t), \widetilde{y}_2(t), \ldots, \widetilde{y}_N(t)) \\ D^{\omega}_{*}\widetilde{y}_2(t) = g_2(t, \widetilde{y}_1(t), \widetilde{y}_2(t), \ldots, \widetilde{y}_N(t)) \\ \vdots & 0 < \omega < 1, \\ D^{\omega}_{*}\widetilde{y}_N(t) = g_N(t, \widetilde{y}_1(t), \widetilde{y}_2(t), \ldots, \widetilde{y}_N(t)) \\ \widetilde{y}_i(0) = \mu_i, i = 1, 2, \ldots, N \end{cases} \tag{16}$$

we consider

$$e_i(t) = y_i(t) - \widetilde{y}_i(t). \tag{17}$$

Is the calculation error of $y(t)$, therefore

$$R_{i,j}(t) = \frac{1}{\Gamma(1-\omega)} \int_0^t (t-\tau)^{-\omega} y'_j(\tau) d\tau - g_i(t, y_1(t), y_2(t), ..., y_N(t)), \tag{18}$$

and

$$\widetilde{R}_{i,j}(t) = \frac{1}{\Gamma(1-\omega)} \int_0^t (t-\tau)^{-\omega} \widetilde{y}'_j(\tau) d\tau - g_i(t, \widetilde{y}_1(t), \widetilde{y}_2(t), ..., \widetilde{y}_N(t)). \tag{19}$$

Subtracting both sides of the Eq. (18) and Eq. (19),we have:

$$\begin{aligned} E_{i,j}(t) = &\frac{1}{\Gamma(1-\omega)} \int_0^t (t-\tau)^{-\omega} e'_j(\tau) d\tau \\ &-[g_i(t, y_1(t), y_2(t), ..., y_N(t)) - g_i(t, \widetilde{y}_1(t), \widetilde{y}_2(t), ..., \widetilde{y}_N(t))]. \end{aligned}$$

We consider

$$
\begin{aligned}
G_i(t, e_1(t), e_2(t), ..., e_N(t)) &= g(t, y(t)) - g(t, y_N(t)) \\
&= g_i(t, y_1(t), y_2(t), ..., y_N(t)) - g_i(t, \widetilde{y}_1(t), \widetilde{y}_2(t), ..., \widetilde{y}_N(t)) \\
&= g_i(t, \widetilde{y}_1(t) + e_1(t), \widetilde{y}_2(t) + e_2(t), ..., \widetilde{y}_N(t) + e_N(t)) \\
&\qquad - g_i(t, \widetilde{y}_1(t), \widetilde{y}_2(t), ..., \widetilde{y}_N(t)).
\end{aligned}
$$

By using the Taylor expansion:

$$
\begin{aligned}
G_i(t, e_1(t), e_2(t), ..., e_N(t)) \simeq e_1(t) &\frac{\partial g_i(t, \widetilde{y}_1(t), \widetilde{y}_2(t), ..., \widetilde{y}_N(t))}{\partial \widetilde{y}_1(t)} \\
+e_2(t) &\frac{\partial g_i(t, \widetilde{y}_1(t), \widetilde{y}_2(t), ..., \widetilde{y}_N(t))}{\partial \widetilde{y}_2(t)} \\
+... + e_N(t) &\frac{\partial g_i(t, \widetilde{y}_1(t), \widetilde{y}_2(t), ..., \widetilde{y}_N(t))}{\partial \widetilde{y}_N(t)},
\end{aligned}
$$

that is

$$
\frac{\partial g_i(t, \widetilde{y}_1(t), \widetilde{y}_2(t), ..., \widetilde{y}_N(t))}{\partial \widetilde{y}_j(t)} = \frac{d g_i(t, \widetilde{y}_1(t), \widetilde{y}_2(t), ..., \widetilde{y}_N(t))}{dt} \times \frac{1}{\frac{d\widetilde{y}_j(t)}{dt}},
$$

Where g_i and $\widetilde{y}_j(t)$ are known functions, then by solving the system of differential equations of the following fraction we can calculate the approximate error:

$$
\begin{cases}
D_*^{\omega} e_1(t) = G_1(t, y_1(t), y_2(t), \dots, y_N(t)) \\
D_*^{\omega} e_2(t) = G_2(t, y_1(t), y_2(t), \dots, y_N(t)) \\
\vdots & 0 < \omega < 1. \\
D_*^{\omega} e_N(t) = G_N(t, y_1(t), y_2(t) \dots, y_N(t)) \\
e_i(0) = 0, i = 1, 2, \dots, N.
\end{cases}
\tag{20}
$$

5. Numerical solution of CD4+T cell HIV infection fractional order model

Human Immunodeficiency Virus (HIV) is a type of lentivirus, which belongs to the broader retrovirus family. It has a near-spherical shape with a diameter of roughly 120 nanometersabout 60 times smaller than a red blood cell. HIV primarily targets and weakens the immune system, making the body vulnerable to infections and diseases like cancer. It specifically attacks CD4+ T cells, a subset of white blood cells that play a critical role in immune defense. If the destruction of CD4+ T cells becomes excessive, the body loses its ability to effectively combat infections and other diseases.

While HIV poses a significant threat to the immune system, early diagnosis and timely intervention can significantly slow or even halt its progression. Antiretroviral medications (ARVs) are effective in managing the virus, allowing the immune system to recover and maintain a better functional state. Monitoring the CD4+ T cell count, both in terms of infected and healthy cells, is crucial in assessing the stage of HIV infection and determining the most effective treatment plan [6, 15].

In recent years, mathematical models have been developed to analyze the dynamics of CD4+ T cell populations and their interaction with HIV, providing deeper insights into the viruss behavior and aiding in the optimization of treatment strategies. The model in [26] is one of them written with a system of differential equations:

$$\begin{cases} \frac{dT}{dt} = q - \eta T + rT(1 - \frac{T+1}{T_{max}}) - kVT \\ \dfrac{dI}{dt} = kVT - \beta I \\ \dfrac{dV}{dt} = \mu\beta I - \xi V \\ T(0) = T_0, I(0) = I_0, V(0) = V_0 \end{cases} \qquad 0 < t < R < \infty. \tag{21}$$

Each of the parameters of this model is described in Table 2. Recently, many mathematicians have studied this model and proposed various numerical methods to solve it. For example,

Table 2. List of variable and parameters [23]

variable	Meaning
$T(t)$	The concentration of non-infected CD4+T cells in the bloodstream.
$I(t)$	The concentration of CD4+T cells infected by HIV in the bloodstream.
$V(t)$	The concentration of HIV viral particles in the bloodstream.
η	Turnover rate of non-infected CD4+T cells.
β	Turnover rate of infected CD+4T cells.
ξ	Turnover rate of HIV particles.
$1 - \frac{T+1}{T_{max}}$	Logistic growth indicator of unifected CD4+T cells
k	The infection rate of CD4+T cells by HIV virus
kVT	Incidence of HIV infection in healthy CD4+ T cells.
μ	The total number of virus particles produced by each infected CD4+ T cell over its entire lifespan.
q	The generation rate of unifected CD4+T cells in the body
$\mu\beta$	The generation rate of virions through infected CD4+T cells
T_{max}	The maximal concentration of CD4+T cells in the blood
r	Tate of cells' duplication through the process of mitosis when they are stimulated by antigen and mitogen

In this paper, we consider the model presented in Eq. (21) as a form of fractional differential equations, so the model changes as follows:

$$\begin{cases} D_*^{\omega} T = q - \eta T + rT(1 - \frac{T+1}{T_{max}}) - kVT \\ D_*^{\omega} I = kVT - \beta I \\ D_*^{\omega} V = \mu\beta I - \xi V \\ T(0) = T_0, I(0) = I_0, V(0) = V_0 \end{cases} \qquad 0 < t < R < \infty, \quad 0 < \omega < 1 \tag{22}$$

The initial values and parameters described in the model are considered as follows: $T_0 = 0.1, I_0 = 0, V_0 = 0.1, q = 0.1, \eta = 0.02, \beta = 0.3, r = 3, \xi = 2.4, k = 0.00027, T_{max} = 1500, \mu = 10$.
In Tables 3 ,4 and 5 we comparison $M = 15, k = 1, \gamma = 1, \omega = 1$.

Table 3. Numerical comparison for $T(t)$

t	Present method	Method in [27]	VIM [19]	LADM-Pade [20]
0	0.1	0.1	0.1	0.1
0.2	0.208808084	0.2038616561	0.2088073214	0.2088072731
0.4	0.406240543	0.3803309335	0.4061346587	0.4061052625
0.6	0.766442390	0.6954623767	0.7624530350	0.7611467713
0.8	1.414046852	1.2759624442	1.3978805880	1.3773198590
1	2.59155948	2.3832277428	2.5067466690	2.3291697610

Table 4. Numerical comparison for $I(t)$

t	Present method	Method in [27]	VIM [19]	LADM-Pade [20]
0	0	0	0	0
0.2	6.03270224e-6	0.6247872100e-5	0.6032634366e-5	0.603270728e-5
0.4	1.31583409e-5	0.1293552225e-4	0.1314878543e-4	0.131591617e-4
0.6	2.12237854e-5	0.2035267183e-4	0.2101417193e-4	0.212683688e-4
0.8	3.01774201e-5	0.2837302120e-4	0.2795130456e-4	0.300691867e-4
1	4.00378155e-5	0.3690842367e-4	0.2431562317e-4	0.398736542e-4

Table 5. Numerical comparison for $V(t)$

t	Present method	Method in [27]	VIM [19]	LADM-Pade [20]
0	0.1	0.1	0.1	0.1
0.2	0.061879843	0.06187991856	0.06187995314	0.06187996025
0.4	0.038294888	0.03829493490	0.03830820126	0.03831324883
0.6	0.023704550	0.02370431860	0.02392029257	0.02439174349
0.8	0.014680364	0.01467956982	0.01621704553	0.009967218934
1	0.009100845	0.02370431861	0.01608418711	0.003305076447

In Figures 2 ,3 and 4 we cpmpare $T(t)$, $I(t)$ and $V(t)$ for $M = 3, k = 1, \gamma = \omega = 0.8, 0.85, 0.9$.

Tables 6, 7 and 8 show the values of $T(t), I(t)$ and $V(t)$, for $M = 15, k = 1, \gamma = \omega = 0.75, 0.80, 0.85, 0.90, 0.95$.

Table 6. The values of $T(t)$ for $M = 15$, $k = 1$ and $\omega = \gamma$

t	$\omega = 0.75$	$\omega = 0.80$	$\omega = 0.85$	$\omega = 0.90$	$\omega = 0.95$	$\omega = 0.98$
0	0.1	0.1	0.1	0.1	0.1	0.1
0.2	0.2157344	0.2272514	0.2501158	0.2790315	0.3165184	0.3670560
0.4	0.4264249	0.4606339	0.5309877	0.6246844	0.7540629	0.9419131
0.6	0.8133480	0.8979687	1.0784967	1.3317891	1.7039759	2.2858520
0.8	1.5242915	1.8178109	2.1489168	2.7836259	3.7737946	5.4360892
1	2.8300579	3.2590105	4.2409152	5.7619568	8.2742007	12.784070

6. Conclusion

The purpose of this work is to present the Müntz wavelet and use it as a basis for solving the system of fractional differential equations. The growth model of the HIV virus is definitely an important application of this method.

To continue our research, I propose solving other problems using this wavelet.

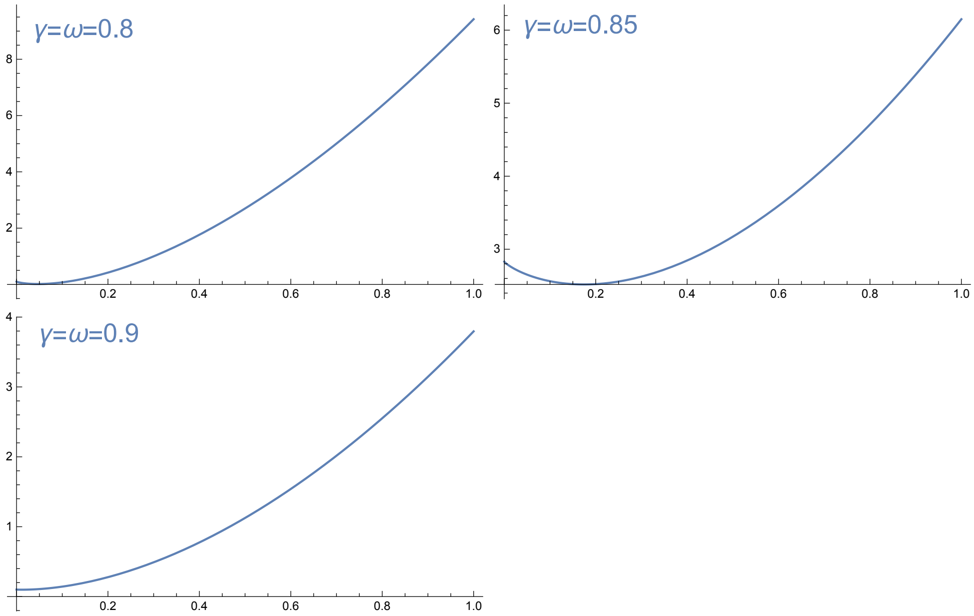

Figure 2. Numerical results for $T(t)$ by $\gamma = \omega = 0.85, 0.9, 0.95$ and $M = 3$ and $k = 1$.

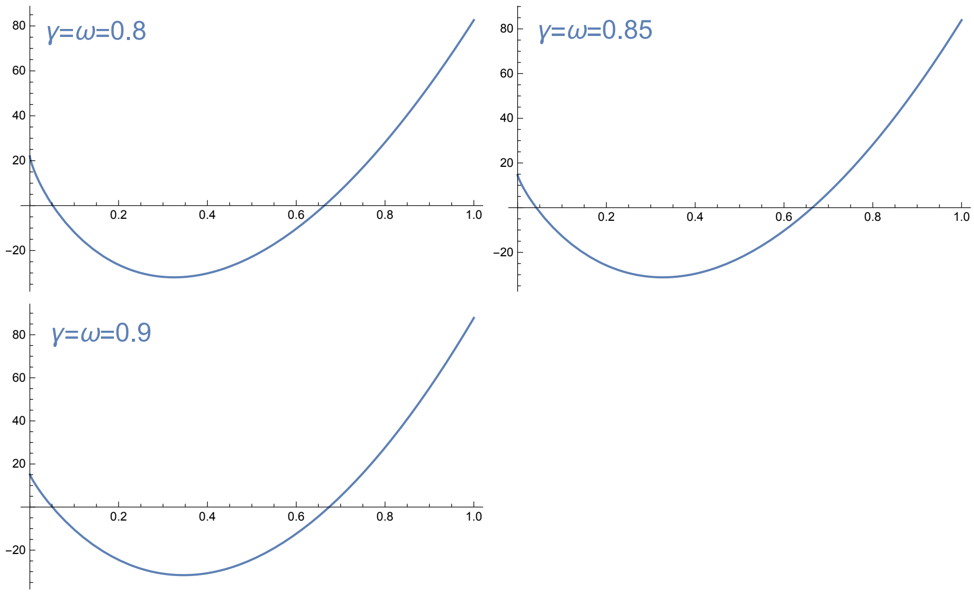

Figure 3. Numerical results for $I(t)$ by $\gamma = \omega = 0.85, 0.9, 0.95$ and $M = 3$ and $k = 1$.

References

[1] R. M. Aiex, I. F. Pierce, G. Donizetti, C. M. von Weber, G. Bizet, C. P. E. Bach, R. Strauss, L. van Beethoven, W. A. Mozart and P. Dukas, Computing tools for modelling orchestral performance, Tech. Rep. DAMTP 2000/NA10, Department of Applied Mathematics and Theoretical Physics, University of Cambridge, Cambridge, UK, (2000).

[2] A. Babaaghaie and K. Maleknejad, Numerical solutions of nonlinear two-dimensional partial Volterra integro-differential equations by Haar wavelet, Journal of Computational and Applied Mathematics, **317** (2017) 643-651.

[3] M. Bahmanpour, M.A.Fariborzi Araghi, Numerical solution of Fredholm and Volterra integral equations of the first kind using wavelets bases, The Journal of Mathematics and Computer Science, **5(4)**

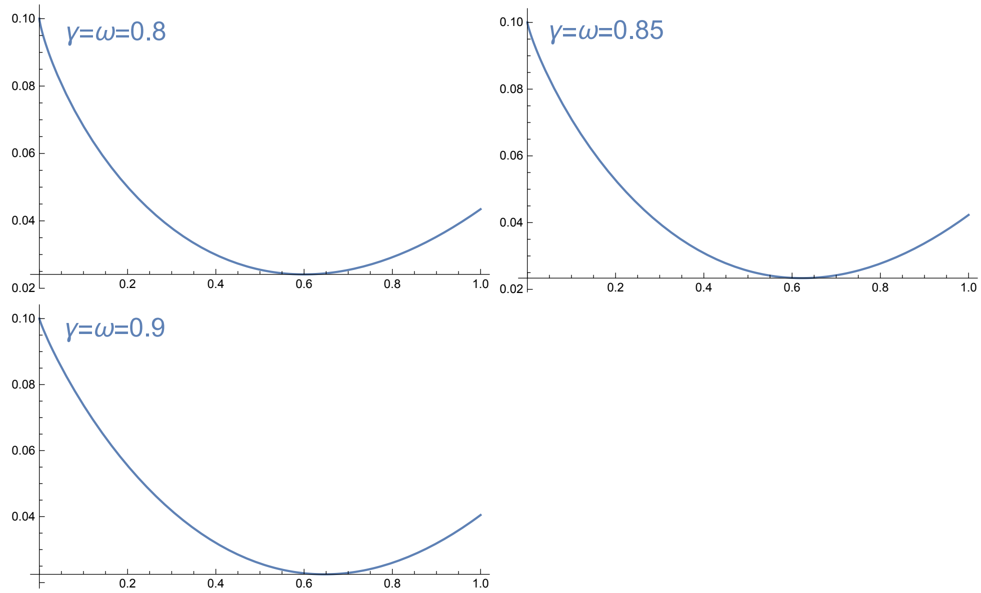

Figure 4. Numerical results for $V(t)$ by $\gamma = \omega = 0.85, 0.9, 0.95$ and $M = 3$ and $k = 1$.

Table 7. The values of $I(t)$ for $M = 15$, $k = 1$ and $\omega = \gamma$

t	$\omega = 0.75$	$\omega = 0.80$	$\omega = 0.85$	$\omega = 0.90$	$\omega = 0.95$	$\omega = 0.98$
0	0	0	0	0	0	0
0.2	6.3363901e-6	6.8290042e-6	7.7692349e-6	8.9043994e-6	1.0315362e-5	1.2151979e-5
0.4	1.3753198e-5	1.4746964e-5	1.6753726e-5	1.9385818e-5	2.2989039e-5	2.8204527e-5
0.6	2.2294605e-5	2.4155672e-5	2.8164952e-5	3.3864401e-5	4.2343235e-5	5.5742298e-5
0.8	3.2111872e-5	3.5585428e-5	4.3464569e-5	5.5403434e-5	7.4433150e-5	1.0695931e-4
1	4.3511235e-5	4.9905893e-5	6.5030221e-5	8.9263409e-5	1.3048453e-4	2.0660978e-4

Table 8. The values of $V(t)$ for $M = 15$, $k = 1$ and $\omega = \gamma$

t	$\omega = 0.75$	$\omega = 0.80$	$\omega = 0.85$	$\omega = 0.90$	$\omega = 0.95$	$\omega = 0.98$
0	0.1	0.1	0.1	0.1	0.1	0.1
0.2	0.0608295	0.0592643	0.0567019	0.0542264	0.0518676	0.0496485
0.4	0.0377472	0.0369869	0.0358789	0.0349582	0.0342057	0.0335988
0.6	0.0237253	0.0237983	0.02401462	0.0243227	0.0246948	0.0251079
0.8	0.0151098	0.0157587	0.0168397	0.0179038	0.0189386	0.0199388
1	0.0097708	0.0107509	0.0123158	0.0137958	0.0151977	0.0165367

(2012) 337-345.

[4] M. Bahmanpour, M.A. Fariborzi Araghi , A method for solving Fredholm integral equation of the first kind based on Chebyshev wavelets, Analysis in Theory and Applications Anal. Theory Appl., **29(3)** (2013) 197-207.

[5] M. Behroozifar , A. Sazmand, An approximate solution based on Jacobi polynomials for time-fractional convection-diffusion equation, Applied Mathematics and Computation,**296(1)** (2017) 1-17.

[6] E.Chorukova, I. Simeonov , A simple mathematical model of the anaerobic digestion of wasted fruits and vegetables in mesophilic conditions, International Journal Bioautomation, **19** (2015) S69-S80.

[7] K. Diethelm, G. Walz, Numerical solution of fractional order differential equations by extrapolation, Numer. Algorithms **16** (1997) 231-253.

[8] A. El-sayed, M. Gaber, The Adomian decomposition method for solving partial differential equations of fractional order in finite domains, Phys. Lett. A, **359** (2006) 175-182.

[9] M.A Friborzi Araghi, M. Bahmanpour, Numerical solution of Fredholm integral equation of the first kind using Legendre, Chebyshev and CAS wavelets, International Journal Of Mathematical Sciences And Engineering Applications, **2(4)**(2008) 1-9.

[10] Fractal functions, fractal surfaces and wavelets (Second Edition) , Academic Press, (2016) 261-327.

[11] L. Galeone, R. Garrappa, On multistep methods for differential equations of fractional order, Mediterr.

J. Math. **3** (2006) 565-580.

[12] R. Garrappa and M. Popolizio, On accurate product integration rules for linear fractional differential equations, J. Comput. Appl. Math. **235** (2011) 1085-1097.

[13] R. Hilfer (Ed.), Applications of fractional calculus in physics, World Scientific Publishing Company, Singapore, (2000).

[14] A. A. Kilbas, H. M. Srivastava and J. J. Trujillo, Theory and applications of fractional differential equations, North-Holland Mathematics Studies, Elsevier Science B.V., Amsterdam, **204** (2006).

[15] N. V.Kumar , L. Mathew, E. G. Wesely , Computational modelling of pisum sativum L. Superoxide dismutase and prediction of mutational variations through in silico methods, International Journal Bioautomation, **18(2)** (2014) 75-88.

[16] M. Lakestani, M. Dehghan, S. Irandoust-Pakchin, The construction of operational matrix of fractional derivatives using B-spline functions, Commun. Nonlinear Sci. Numer. Simul. **17** (2012) 1149-1162.

[17] K. S. Miller and B. Ross, An introduction to the fractional calculus and fractional differential equations, A Wiley-Interscience Publication, John Wiley and Sons, New York, Chichester, Brisbane and Toronto, (1993).

[18] Yi-Ming Chen, Yan-Qiao Wei , Da-Yan Liub, Hao Yua , Numerical solution for a class of nonlinear variable order fractional differential equations with Legendre wavelets, Applied Mathematics Letters, **46** (2015) 83-88.

[19] M. Merdan , A. Gokdogan, A. Yildirim, On the numerical solution of the model for HIV infection of CD4+T cells, Computers and Mathematics with Applications, **62(1)** (2011) 118-123.

[20] M. Y.Ongun ,The laplace Adomian decomposition method for solving a model for HIV infection of CD4+T cells, Mathematical and Computer Modelling, **53(6)** (2011) 597- 603.

[21] I. Podlubny, Fractional differential equations: An introduction to fractional derivatives, fractional differential equations, to methods of their solution and some of their applications, Mathematics in Science and Engineering, Academic Press, New York, London and SanDiego,**198** (1999).

[22] B. Ross, The development of fractional calculus 1695-1900, Hist. Math. **4 (1)** (1977) 75-89.

[23] M. Rasouli Gandomani, M. Tavassoli Kajani, Numerical solution of a fractional order model of HIV infection of CD4+T cells using Mntz-Legendre polynomials, INT.J.BIOAUTOMATION,**20(2)** (2016) 193-204.

[24] M. Rasouli Gandomani1, M. Tavassoli Kajani ,Application of shifted Müntz-legendre polynomials for solving fractional differential equations , International Journal of Pure and Applied Mathematics, **103 (2)** (2015) 263-279.

[25] Y.A. Rossikhin, M.V. Shitikova, Application of fractional calculus for dynamic problems of solid mechanics: novel trends and recent result, Appl. Mech.Rev. **63 (2010)** 52 pages.

[26] L. Wang , M. Y. Li , Mathematical analysis of the global dynamics of a model for HIV infection of CD4+T cells, Mathematical Biosciences. **200(1)** (2006) 44-57.

[27] S.Yuzbasi , A numerical approach to solve the model for HIV infection of CD4+T cells, Applied Mathematical Modelling, **36(12)** (2012) 5876-5890.